

The Entropy Generation Analysis with Interaction of Nanofluid for Metachronal Waves of Cilia



By

Muhammad Shoaib

Department of Mathematics,

School of Natural Sciences (SNS),

National University of Sciences and Technology (NUST),

Islamabad, Pakistan.

2015

The Entropy Generation Analysis with Interaction of Nanofluid for Metachronal Waves of Cilia

By

Muhammad Shoaib



A dissertation submitted in partial fulfillment of the requirements
for the degree of Master of Philosophy in Mathematics

Supervised by

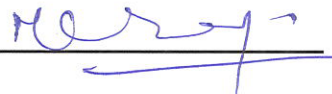
Dr. Noreen Sher Akbar

Department of Mathematics,
School of Natural Sciences (SNS),
National University of Sciences and Technology (NUST),
Islamabad, Pakistan.

2015

National University of Sciences & Technology**M.Phil THESIS WORK**

We hereby recommend that the dissertation prepared under our supervision by: MUHAMMAD SHOAIB, Regn No. NUST201361937MSNS78013F Titled: Entropy Generation Analysis with the Interaction of Nanofluid for Metachronal Waves of Cilia be accepted in partial fulfillment of the requirements for the award of **M.Phil** degree.

Examination Committee Members1. Name: Dr. Meraj Mustafa HashmiSignature: 2. Name: Dr. Asim AzizSignature: 3. Name: Dr. Muhammad Mudassir GulzarSignature: 4. Name: Dr. Sohail NadeemSignature: Supervisor's Name: Dr. Noreen Sher AkbarSignature: Head of Department08/9/15Date**COUNTERSIGNED**Date: 08/09/15
Dean/Principal

*Dedicated to
my respected parents,
my loving sisters
and brothers*

Acknowledgements

Almighty Allah is very kind and compassionate, gives power to the weak and helps the helpless, the most Gracious and Merciful.

I would like to express my sincere gratitude to my supervisor Dr. Noreen Sher Akbar, for her valuable suggestions, support, guidance and encouragement throughout my research work and dissertation.

I also wish to express my appreciation to the Principal of School of Natural Sciences (SNS), National University of Sciences and Technology, Islamabad, Prof. Azad Akhter Siddiqui, Head of the Mathematics Department Dr. Rashid Farooq, Head of Research Dr. Tooba Siddiqui for their valuable support and efforts for the students of the department.

I am thankful to the guidance of examination committee (GEC) members Dr. Asim Aziz (CEME), Col. Dr. Muhammad Mudassar Gulzar, TI(M) (CEME) and Dr. Meraj Mustafa Hashmi (SNS).

I am extremely grateful to all the faculty members especially, Prof. Faiz Ahmad, Dr. Muhammad Asif Farooq, Dr. Yousaf Habib, Dr. Mujeeb-ur-Rehman, Dr. Muhammad Imran, Dr. Matloob Anwar, Dr. Muhammad Ishaq, Dr. Mubasher Jamil and Dr. Moniba Shams for their help and encouragement.

I am thankful to all my seniors, class fellows and friends for their help and support at different stages and making my time memorable.

This acknowledgement would be incomplete without expressing my special thanks to my family members, especially to my parents, brothers and sisters.

Finally, I would like to thank, all the staff members of SNS for their kindness.

Muhammad Shoab

Abstract

The most important things which are studied in fluid dynamics are fluid's velocity, temperature, pressure and momentum. The current systemic study is associated with the study of viscous flow in ciliated tube with permeable walls and entropy generation analysis. Initially, the mathematical model of copper nanofluids with Pure water as the base fluid, has been formulated in the form of non-linear partial differential equations. These are then transformed to a system of ordinary differential equations using the dimensionless variables and the conditions of low Reynolds number and long wavelength approximation. Exact solutions have been evaluated for the transformed ODEs for temperature, velocity and pressure gradient. The graphs are also plotted for better understanding and analysis of the solution.

Contents

1	Introduction	4
2	Preliminaries	7
2.1	Fluid	7
2.2	Fluid Mechanics	7
2.2.1	Fluid Statics	7
2.2.2	Fluid Kinematics	7
2.2.3	Fluid Dynamics	8
2.3	Viscosity (Dynamic Viscosity)	8
2.4	Types of Fluids	8
2.4.1	Ideal Fluids	8
2.4.2	Real Fluids	8
2.4.3	Incompressible Fluids	9
2.4.4	Compressible Fluids	9
2.5	Newton's Law of Viscosity	9
2.5.1	Newtonian Fluids	9
2.5.2	Non-Newtonian Fluids	9
2.6	Time Independent Fluids	10
2.6.1	Plastics	10
2.6.2	Pseudoplastics (Shear Thinning)	10
2.6.3	Dilatent (Shear Thickening)	10
2.7	Time Dependent Fluids	11

2.7.1	Thixotropic	11
2.7.2	Rheopectic	11
2.7.3	Density	11
2.8	Methods of Description (Motion of Fluid Particle)	11
2.8.1	Langrangian Method	11
2.8.2	Eulerian Method	11
2.9	Types of Flow	12
2.9.1	Uniform Flow	12
2.9.2	Non-uniform Flow	12
2.9.3	Laminar Flow	12
2.9.4	Turbulent Flow	12
2.9.5	Steady Flow (Time Independent Flow)	12
2.9.6	Unsteady Flow (Time Dependent Flow)	12
2.9.7	Incompressible Flow	12
2.9.8	Compressible Flow	13
2.9.9	Irrotational Flow	13
2.9.10	Rotational Flow	13
2.10	Flow Patterns	13
2.10.1	Streamline	13
2.10.2	Stream Function (ψ)	13
2.11	One-dimensional Flow	14
2.12	Two-dimensional Flow	14
2.13	Volume Flow Rate	15
2.14	Continuity Equation	15
2.15	Momentum Equation	15
2.16	Energy Equation	16
2.17	Nanofluids	16
2.18	Nanoparticles	16
2.19	Base Fluids	16
2.20	Carbon Nanotubes	16

2.21	Cilia	17
2.22	Grashof Number	17
2.23	Hartmann Number	18
2.24	Reynolds Number	18
2.25	Prandtl Number	18
2.26	Eckert Number	19
2.27	Brinkman Number	19
2.28	Darcy Number	19
3	CNT Suspended Nanofluid Analysis in a Flexible Tube with Ciliated Walls	20
3.1	Introduction	20
3.2	Formulation of the Problem	21
3.3	Solutions of the Problem	25
3.4	Results and Discussion	26
3.5	Conclusion	30
4	A Study of Entropy Generation and Heat Transfer for CNT Suspended Nanofluid in a Porous Ciliated Tube with Permeable Walls	32
4.1	Introduction	32
4.2	Formulation of the Problem	33
4.3	Analytic Solutions	35
4.4	Entropy Generation	36
4.5	Results and Discussion	36
4.6	Conclusion	45

Chapter 1

Introduction

In past decades, nanofluids have been receiving much attention in science, engineering, medical (targeted drug delivery) and industry since its discovery owing to its enhanced thermal conductivity and heat transfer characteristics which makes them a promising heat exchangers, cooling devices and solar collectors in heat transfer application. Nanofluids are fabricated by dispersing of nanoparticles (Al_2O_3 , CuO , TiO_2 and CNT etc) in base fluids, such as water, ethylene glycol and oil etc. Some investigators [1-3] are considering carbon nanotubes (CNT) in synthesizing the nanofluids due to its high thermal conductivity in comparison to other nanoparticles. CNTs are basically being used in the form of single-wall CNT, double-wall CNT and multi-wall CNT. Xie and Chen [4] have reviewed on the preparation techniques, the experimental and theoretical studies on the heat transfer characteristics of CNT nanofluids have concluded that thermal conductivity of CNTs, interfacial thermal resistance between the CNT and the matrix, and dispersion status of the CNTs in the base fluid have significant effects on the thermal transport in the CNT nanofluids due to the complex morphologies and surface chemistry of the suspended CNTs. Another review on CNT nanofluids has been presented by Murshed and Castro [5] and concluded that nanofluids containing multi-wall carbon nanotubes (MWCNT) are found to exhibit higher conductivity and heat capacity compared to base ionic liquids. Recently, much attention has been focused on the study of CNT in nanofluids: Halelfadl et al. [6], Saida et al. [7], Hordy et al. [8], Yadav et al.[9], Walvekara et al. [10] and Xing et al. [11] have discussed the efficiency, stability and thermos-physical property of CNTs. Very recently akbar and Butt[12] presented "CNT suspended nanofluid analysis in a flexible with ciliated walls".

In past decades, much attention was focused on natural propulsion mechanisms (Lardner and Shack [13], Sleight [14 & 15] and Blake [16 & 17]) by the expulsion of mucus from the lungs due to hair-like structures, called cilia, that cover the inner layer of the mammalian trachea. They propel a relatively larger volume of fluid during the effective stroke when compared with the recovery stroke and therefore create a net fluid transport in the direction of the effective stroke. In same fashion, Khaderi et al. [18] studied the breaking of symmetry in microfluidic propulsion driven by artificial cilia. Khaderi et al. [19] further reported for microfluidic propulsion by the metachronal beating of magnetic artificial cilia, a numerical analysis and Khaderi and Onck [20] extended their earlier work for the fluid structure interaction of three-dimensional magnetic artificial cilia.

The first law of thermodynamics states that the energy is conserved however the second law states that there is entropy due to irreversibility of natural process [21]. Since the quality of energy (exergy) decreases due to entropy. So that to maintain the energy quality, it is required to control the entropy generation during the convective fluid flow. A study of entropy generation in convective heat transfer for different flow configurations: pipe flow, boundary layer over flat plate, single cylinder in cross-flow, flow in the entrance region of a flat rectangular duct has been studied by Bejan [22] and derived a non-dimensional number (Bejan Number) which is the ratio of the entropy generation due to the heat transfer to the total entropy generation. Further Bejan [23] extended his study for counter flow heat exchangers for gas-gas applications. Bejan [24] again introduced the new thermodynamics of finite-size devices and finite-time processes to minimize the entropy generation. Baytas [25] incorporated the Darcy's law in his study and discussed the entropy generation for natural convection in an inclined porous cavity. In addition to above studies, Tasmin et al. [26] generalized for hydromagnetic effect for entropy generation in porous channel. Mahmud and Fraser [27] extended for entropy generation in a square porous cavity with magnetohydrodynamics free convection. Earlier works in this context involved the study of natural convection heat transfer mechanism with porosity and magnetohydrodynamics effects. But in past few decades the application of nanofluids in convective heat transfer is more attractive for researchers to study the entropy generation. Further analysis related to the topic can be seen through Refs. [28-36].

In all above investigations, there is no study of combined effects of CNT-nanofluids, entropy

generation and cilia motion, which is an essential application in manufacturing the microfluidic devices and artificial cilia. In continuation of above studies, a mathematical model to study the entropy generation, heat transfer and metachronal wave propulsion due to beating cilia is investigated in this thesis. So we organized thesis as follows: In chapter 2 presented the basic definitions. In chapter 3 CNT suspended nanofluid analysis in a flexible tube with ciliated walls is presented. Chapter 4 presents a study of entropy generation and heat transfer of CNT-nanofluids in flow driven by beating cilia through porous medium.

Chapter 2

Preliminaries

2.1 Fluid

Fluid is a substance which deforms continuously under the action of shearing forces, no matter how small they may be. Basically fluids are divided into two groups.

- (1) Liquids
- (2) Gases

2.2 Fluid Mechanics

The study of the behaviors of fluids such as liquids and gases at rest or in motion is called fluid mechanics. It is divided into following sub-categories.

- (1) Fluid statics
- (2) Fluid kinematics
- (3) Fluid dynamics

2.2.1 Fluid Statics

The study of fluids at rest is called fluid statics.

2.2.2 Fluid Kinematics

The study of fluids in motion without considering any kind of force which causes the motion is called Fluid kinematics.

2.2.3 Fluid Dynamics

The study of fluids in motion considering forces which are acting on the fluids is called fluid dynamics or fluid kinetics. In this sense we can define fluid as the substance which deforms continuously under the action of shearing forces.

2.3 Viscosity (Dynamic Viscosity)

It is physical property of the fluid associated with shearing deformation of fluid particles under the action of applied forces. In short, it can be defined as the internal resistance to the flow of fluid. It can also be defined as the ratio between shear stress τ and velocity gradient or deformation rate du/dy . Mathematically written as

$$\mu = \frac{\tau}{\frac{du}{dy}}. \quad (2.1)$$

It's S.I unit is Pascal-second (pa.s) or kg/m.s.

2.4 Types of Fluids

Following are the main types of fluids. (1) Ideal fluids (2) Real fluids (3) Incompressible fluids (4) Compressible fluids

2.4.1 Ideal Fluids

Those fluids which have zero viscosity (μ) are called ideal fluids, i.e

$$\mu = 0.$$

2.4.2 Real Fluids

Those fluids which have non-zero viscosity (μ) are called real fluids, i.e

$$\mu \neq 0.$$

For example: Honey, ketchup etc.

2.4.3 Incompressible Fluids

Incompressible fluid is a fluid that does not change the volume of the fluid due to external pressure is called incompressible fluids. For example, water, oil etc.

2.4.4 Compressible Fluids

If the volume of fluid changes due to external pressure is called compressible fluids. For example, the air flowing up to 120 mile/hour.

2.5 Newton's Law of Viscosity

The relation between shear stress and shear rate is defined as Newton's law of viscosity, shear stress is directly proportional to shear rate. Mathematically

$$\tau = \mu \frac{du}{dy}, \quad (2.2)$$

here τ is the shear stress, μ is constant of proportionality known as dynamic viscosity and du/dy is the deformation rate.

2.5.1 Newtonian Fluids

Those fluids which obey the Newton's law of viscosity are called Newtonian fluids.

Note: Water and most gases are Newtonian.

2.5.2 Non-Newtonian Fluids

Those fluids which do not obey the Newton's law of viscosity are called non-Newtonian fluids.

In Newtonian fluids, the shear stress τ is linearly proportional to shear rate du/dy , while in non-Newtonian fluids the shear stress τ is non-linearly proportional to shear rate du/dy . Mathematically

$$\tau = K \left(\frac{du}{dy} \right)^n. \quad (2.3)$$

Here " K " is consistency index and " n " is flow behaviors index. If $n=1$ and $K=\mu$ then it represents Newtonian fluids.

The general mathematical form of non-Newtonian fluid is

$$\tau = \eta \frac{du}{dy}, \quad (2.4)$$

here

$$\eta = \mu \left(\frac{du}{dy} \right)^{n-1}, \quad (2.5)$$

known as apparent viscosity. Here in non-Newtonian fluids, the viscosity (apparent) is dependent on shear stress, but in Newtonian fluids the dynamic viscosity (μ) is independent of shear stress and is constant.

2.6 Time Independent Fluids

2.6.1 Plastics

Plastics for which shear stress must reach to a minimum value before the flow commences, thereafter, shear stress increases with the rate of shear strain. For example: Sewage sludge, Toothpaste etc.

2.6.2 Pseudoplastics (Shear Thinning)

Those fluids for which the apparent viscosity (η) decreases with increasing deformation rate. Examples are cement, blood etc.

Note: For pseudoplastics $n < 1$ in Eq. 2.5.

2.6.3 Dilatent (Shear Thickening)

Those substance in which apparent viscosity (η) increases with decreasing deformation rate. Examples are butter, quicksand etc.

Note: For dilatent $n > 1$ in Eq. 2.5.

2.7 Time Dependent Fluids

2.7.1 Thixotropic

Fluids for which apparent viscosity (η) decreases with time under constant applied shear stress are called thixotropic fluids. For example, Paints.

2.7.2 Rheopectic

Fluids for which apparent viscosity (η) increases with time under constant applied shear stress are called rheopectic fluids. Examples are printer ink, gypsum paste, lubricants etc.

2.7.3 Density

The density of a fluid is defined as its mass per unit volume. It is denoted by the Greek symbol, ρ . If the density is constant (most liquids), the flow is incompressible. If the density varies significantly (e.g some gas flows), the flow is compressible.

2.8 Methods of Description (Motion of Fluid Particle)

A fluid consists of countless particles, whose relative positions are never fixed. Whenever a fluid is in motion, these particles move along certain lines, depending upon the type of fluid as well as shape of the path through which the fluid particles move. For mathematical analysis of the fluid motion, following two methods are commonly used:

1. Lagrangian method.
2. Eulerian method.

2.8.1 Lagrangian Method

This method deals with the study of flow pattern of the individual particles. In this method, the particle traced the path under consideration with the passage of time.

2.8.2 Eulerian Method

This method deals with the study of flow pattern of all the particles at fixed section. The path traced by all the particles at fixed section and time are studied by this method.

2.9 Types of Flow

2.9.1 Uniform Flow

The flow in which the velocity of fluid particles at all sections of the channel is same is called uniform flow. Flow through a pipe having same diameter at both ends is the example of uniform flow.

2.9.2 Non-uniform Flow

The flow in which the velocity of fluid particles at all sections of the channel is not same is called non-uniform flow. flow through a pipe which has different diameters at the end points is an example of non-uniform flow.

2.9.3 Laminar Flow

A flow in which each fluid particle has definite path and path of individual particles do not cross each other.

2.9.4 Turbulent Flow

A flow in which each fluid particles moves in random motion.

2.9.5 Steady Flow (Time Independent Flow)

The flow in which the velocity of fluid particles at every point does not change with time is called steady flow.

2.9.6 Unsteady Flow (Time Dependent Flow)

The flow in which the velocity of fluid particles at any point changes with time is called unsteady flow.

2.9.7 Incompressible Flow

The flow in which the density remains constant is called incompressible flow.

i.e $\rho = \text{constant}$.

2.9.8 Compressible Flow

The flow in which the density is not constant is called compressible flow.

i.e $\rho \neq \text{constant}$.

2.9.9 Irrotational Flow

Irrotational flow is that type of flow in which the fluid particles do not rotate about their own axis. Mathematically, it is defined as

$$\nabla \times \mathbf{V} = 0. \quad (2.6)$$

2.9.10 Rotational Flow

Rotational flow is a flow in which the fluid particles also rotate about their own axis, while flowing. Mathematically, it can be defined as

$$\nabla \times \mathbf{V} \neq 0. \quad (2.7)$$

2.10 Flow Patterns

We define flow patterns such as, streamlines, pathlines and streaklines in this section.

2.10.1 Streamline

Streamline is a curve that is instantaneously tangent to the velocity vector. In unsteady flow, the streamlines pattern change with time, while in steady flow, the streamlines are fixed in space.

2.10.2 Stream Function (ψ)

It describes the form of flow pattern. It is a mathematical expression that describes the flow field in terms of either mass flow rate for compressible fluids, or volume flow rate for incompressible

fluids. For steady-state two dimensional flow field, we may write

$$\psi = f(x, y) \tag{2.8}$$

here ψ is a stream function and x, y are coordinates of the points.

For incompressible flow, the continuity equation is expressed as

$$\nabla \cdot \mathbf{V} = 0,$$

using the velocity field

$$\mathbf{V} = [u(x, y), v(x, y), 0]$$

we have

$$\frac{\partial u}{\partial x} + \frac{\partial v}{\partial y} = 0.$$

This equation is satisfied identically if a function (ψ) is defined as

$$u = \frac{\partial \psi}{\partial y}, \quad v = -\frac{\partial \psi}{\partial x}.$$

2.11 One-dimensional Flow

One dimensional flow is that type of flow which depends only on one space variable.

For example: (1) $\vec{V} = ax^2i + bxj$.

(2) The steady flow between two concentric rotating cylinders depend only on r -component of velocity.

2.12 Two-dimensional Flow

That type of flow which depends on any two space variables.

For example: $\vec{V} = axi - byj$. or $\vec{V} = (ax + t)i - by^2j$.

2.13 Volume Flow Rate

The flow rate or discharge flow rate of a fluid is the volume of fluid which passes through a surface per unit time. Symbolically, it is represented by Q . It can be expressed in either terms of cross sectional area and velocity, or volume and time. Mathematically can be written as

$$Q = \frac{V}{t}, \quad (2.9)$$

or

$$Q = \vec{v} * a. \quad (2.10)$$

Here V is the Volume of fluid, t is time, \vec{v} is the velocity of the fluid and a is the area of the cross section of the space the fluid is moving through.

2.14 Continuity Equation

Continuity equation is constructed by Law of conservation of mass. The well known continuity equation is

$$\frac{\partial \rho}{\partial t} + \nabla \cdot (\rho \vec{V}) = 0. \quad (2.11)$$

For incompressible fluid it becomes

$$\nabla \cdot \vec{V} = 0.$$

2.15 Momentum Equation

The momentum equation is a statement of Newton's Second Law and relates the sum of the forces acting on an element of fluid to its acceleration or rate of change of momentum. Mathematically it can be expressed as follows

$$\rho \frac{D\vec{V}}{Dt} = \nabla \cdot S + \rho b, \quad (2.12)$$

here $\frac{D}{Dt}$ is material derivative, S is stress tensor and b is body forces.

2.16 Energy Equation

The well known energy equation is

$$\rho c_p \frac{DT}{Dt} = K \nabla^2 T + t_r(\tau L). \quad (2.13)$$

Here c_p is the specific heat, K is thermal conductivity, T is the temperature, τ is tensor and L is dissipation term.

2.17 Nanofluids

Nanofluids are potential heat transfer fluids with enhanced thermophysical properties and heat transfer performance which can be applied in many devices for better performances (i.e. energy, heat transfer and other performances). Nanofluids are the class of fluids which consist of base fluids along with suspended nanoparticles having nanometer size and having diameter less than $100nm$.

2.18 Nanoparticles

Nanoparticles are used in nanofluids. They actually made up of metals (Cu , Al , Ag), oxides ceramics(Al_2O_3 , CuO), nitride ceramics (AlN , SiN), carbide ceramics(SiC , tiC) and carbon nanotubes.

2.19 Base Fluids

Common base fluids are water, oil and ethylene glycol.

2.20 Carbon Nanotubes

Carbon nanotubes ($CNTs$) are hollow cylindrical nanostructures with the walls formed by thick sheets of carbon. They have a very small diameter-to-length ratio. Aside from their extraordinary thermal conductivity, electrical and mechanical properties, carbon nanotubes

find applications as additives to various structural materials including car parts. Nanotubes are classified as single-walled nanotubes (*SWNTs*) and multi-walled nanotubes (*MWNTs*). Single-walled nanotubes have a diameter close to 1 nanometer, and a tube length that can be millions times longer. The structure of a (*SWNT*) may be imagined by wrapping a one-atom-thick layer of graphite into seamless cylinder. Electrical conductivity of (*SWNTs*) can be show metallic or semiconducting behavior. A useful application of (*SWNTs*) is in the development of the first intermolecular field-effect transistors. The multi-walled nanotubes are multiple concentric nanotubes precisely nested within one another and their individual shells described as (*SWNTs*).

2.21 Cilia

Cilia are hair-like structures that protrude from the surfaces of certain organisms and deform in a wavelike fashion to transport fluids. They are present in almost all groups of the animal kingdom because their motility plays a crucial role in certain physiological processes such as respiration, reproduction, locomotion and circulation. These hair-like appendages beat or move in a whip-like asymmetric manner consisting of an effective stroke and recovery stroke. Moreover, when a group of cilia operate together, they beat with a constant phase-lag with their neighbors. This leads to the formation of metachronal waves which are known to enhance the fluid flow due to cilia.

2.22 Grashof Number

The Grashof number is a dimensionless number, denoted by G_r , which is defined as the ratio of the buoyancy force to the viscous force (μ) acting on a fluid. Mathematically

$$G_r = \frac{\text{Buoyancy force}}{\text{Viscous force}}.$$

2.23 Hartmann Number

The Hartmann number is a dimensionless number, denoted by M , which is defined as the ratio of the electromagnetic force to the viscous force (μ) acting on a fluid. Mathematically

$$M = \frac{\text{Electromagnetic force}}{\text{Viscous force}}.$$

2.24 Reynolds Number

Reynolds number is used to check whether the flow is laminar or turbulent, denoted by Re . It is the ratio of inertial force to Viscous force. Mathematically

$$Re = \frac{\rho u L}{\mu}, \quad (2.14)$$

here u is the mean flow velocity of fluid, L is diameter of pipe, ρ is the density of fluid and μ is the fluid viscosity.

2.25 Prandtl Number

Prandtl number Pr is defined as the ratio of momentum diffusivity to thermal diffusivity. Mathematically it can be expressed as

$$Pr = \frac{\nu}{\alpha} = \frac{c_p \mu}{k}, \quad (2.15)$$

as

$$\nu = \frac{\mu}{\rho}, \quad \alpha = \frac{k}{\rho c_p}.$$

Here α is the thermal diffusivity, μ is the dynamic viscosity, k is the thermal conductivity, c_p is the specific heat and ρ is the density of fluid.

2.26 Eckert Number

Eckert number Ec is dimensionless number. It is defined as

$$Ec = \frac{u^2}{c_p \Delta T}, \quad (2.16)$$

here u is the local flow velocity, c_p is the specific heat and ΔT is the difference between wall temperature and local bulk temperature.

2.27 Brinkman Number

Brinkman number (Br) is dimensionless number related to the ratio of heat produced by viscous dissipation and heat transported by molecular conduction. It can also be defined as

$$Br = \frac{\mu u^2}{k (T_w - T_0)} = \text{Pr} \cdot Ec. \quad (2.17)$$

Here μ is the dynamic viscosity, u is the flow velocity, k is the thermal conductivity, T_0 is the bulk fluid temperature, T_w is the wall temperature, Pr is the Prandtl number and Ec is the Eckert number.

2.28 Darcy Number

Darcy number (Da) is dimensionless number defined as the ratio of permeability of the medium to cross-sectional area (commonly the diameter squared).

Mathematically

$$Da = \frac{K}{d^2}, \quad (2.18)$$

here K is the permeability of the medium and d is diameter.

Chapter 3

CNT Suspended Nanofluid Analysis in a Flexible Tube with Ciliated Walls

3.1 Introduction

This chapter is carried out to analyze the effect of heat transfer in a flexible tube with ciliated walls and carbon nanotubes. The problem has been formulated in the form of non linear partial differential equations, which are then reduced to ordinary differential equation form using the dimensionless variables and the condition of low Reynold's number and long wavelength approximation. Exact solutions have been obtained for velocity, temperature, pressure gradient and graphs for velocity, temperature and pressure gradient have been plotted for better analysis

of the solution and physical interpretation.

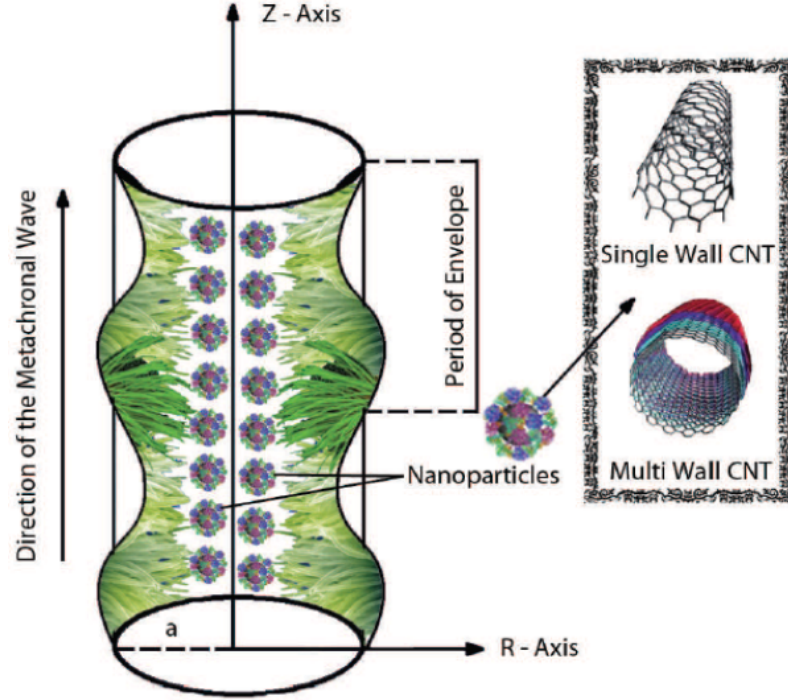


Fig. 3.1. Geometry of the problem

3.2 Formulation of the Problem

Here we consider an axisymmetric vertical tube filled with an incompressible two dimensional and two directional carbon nanotubes suspended nanofluid. Length of the tube is L . The inner surface of the tube is ciliated and the flow is generated due to collective beating of cilia. We choose a cylindrical coordinate system (\bar{R}, \bar{Z}) , where \bar{Z} - axis lies along the centerline of the tube and \bar{R} - axis is normal to it. Cilia deform in a wave-like fashion, an infinite symplectic metachronal wave train is produced which travels with a velocity c along the wall of the tube.

Keeping in view the geometry of the metachronal wave pattern, it is assumed that the envelope of cilia tips can be expressed mathematically in the following form [13 – 15]

$$\bar{R} = \bar{H} = \bar{f}(\bar{Z}, \bar{t}) = a + a\epsilon \cos\left(\frac{2\pi}{\lambda}(\bar{Z} - c\bar{t})\right), \quad (3.1a)$$

which can also be taken as the equation for the extensible boundary of the flow channel. Based

upon different patterns of cilia motion observed by Saleigh [14, 15], the cilia tips can be considered to move in elliptical paths such that the horizontal positions of the cilia tips can be written as [13 – 15]

$$\bar{Z} = \bar{g}(\bar{Z}, \bar{Z}_0, \bar{t}) = a + a\epsilon\alpha \sin\left(\frac{2\pi}{\lambda}(\bar{Z} - c\bar{t})\right), \quad (3.1b)$$

here a denotes the mean radius of the tube, ϵ is the non-dimensional measure with respect to the cilia length, λ and c are the wavelength and wave speed of the metachronal wave respectively. \bar{Z}_0 is the reference position of the particle and α is the measure of the eccentricity of the elliptical motion. If no slip condition is applied, then the initial velocities of the transporting fluid are just those caused by the cilia tips, which can be given as:

$$\bar{W}_0 = \left. \frac{\partial \bar{Z}}{\partial \bar{t}} \right|_{\bar{Z}_0} = \frac{\partial \bar{g}}{\partial \bar{t}} + \frac{\partial \bar{g}}{\partial \bar{Z}} \frac{\partial \bar{Z}}{\partial \bar{t}} = \frac{\partial \bar{g}}{\partial \bar{t}} + \frac{\partial \bar{g}}{\partial \bar{Z}} \bar{W}_0. \quad (3.2a)$$

$$\bar{U}_0 = \left. \frac{\partial \bar{R}}{\partial \bar{t}} \right|_{\bar{Z}_0} = \frac{\partial \bar{f}}{\partial \bar{t}} + \frac{\partial \bar{f}}{\partial \bar{Z}} \frac{\partial \bar{Z}}{\partial \bar{t}} = \frac{\partial \bar{f}}{\partial \bar{t}} + \frac{\partial \bar{f}}{\partial \bar{Z}} \bar{W}_0. \quad (3.2b)$$

Eqs. (3.1) and (3.2) together imply:

$$\bar{W}_0 = \frac{-\frac{2\pi}{\lambda}(\epsilon\alpha a c \cos(\frac{2\pi}{\lambda})(\bar{Z} - c\bar{t}))}{1 - \frac{2\pi}{\lambda}(\epsilon\alpha a \cos(\frac{2\pi}{\lambda})(\bar{Z} - c\bar{t}))}, \quad (3.3a)$$

$$\bar{U}_0 = \frac{\frac{2\pi}{\lambda}(\epsilon a c \sin(\frac{2\pi}{\lambda})(\bar{Z} - c\bar{t}))}{1 - \frac{2\pi}{\lambda}(\epsilon\alpha a \cos(\frac{2\pi}{\lambda})(\bar{Z} - c\bar{t}))}. \quad (3.3b)$$

The governing equations for the flow of an incompressible nanofluid can be written as

$$\frac{1}{\bar{R}} \frac{\partial(\bar{R}\bar{U})}{\partial \bar{R}} + \frac{\partial \bar{W}}{\partial \bar{Z}} = 0, \quad (3.4)$$

$$\begin{aligned} \rho_{nf} \left[\bar{U} \frac{\partial \bar{U}}{\partial \bar{R}} + \bar{W} \frac{\partial \bar{U}}{\partial \bar{Z}} \right] &= -\frac{\partial \bar{P}}{\partial \bar{R}} + \mu_{nf} \frac{\partial}{\partial \bar{R}} \left[2 \frac{\partial \bar{U}}{\partial \bar{R}} \right] + \mu_{nf} \frac{2}{\bar{R}} \left(\frac{\partial \bar{U}}{\partial \bar{R}} - \frac{\bar{U}}{\bar{R}} \right) \\ &\quad + \mu_{nf} \frac{\partial}{\partial \bar{Z}} \left[\left(\frac{\partial \bar{U}}{\partial \bar{R}} + \frac{\partial \bar{W}}{\partial \bar{Z}} \right) \right], \end{aligned} \quad (3.5)$$

$$\begin{aligned} \rho_{nf} \left[\bar{U} \frac{\partial \bar{W}}{\partial \bar{R}} + \bar{W} \frac{\partial \bar{W}}{\partial \bar{Z}} \right] &= -\frac{\partial \bar{P}}{\partial \bar{Z}} + \mu_{nf} \frac{\partial}{\partial \bar{Z}} \left[2 \frac{\partial \bar{W}}{\partial \bar{Z}} \right] + \mu_{nf} \frac{1}{\bar{R}} \frac{\partial}{\partial \bar{R}} \left[\bar{R} \left(\frac{\partial \bar{U}}{\partial \bar{Z}} + \frac{\partial \bar{W}}{\partial \bar{R}} \right) \right] \\ &\quad - \sigma B_o^2 \bar{W} + \rho_{nf} g \alpha (\bar{T} - T_0), \end{aligned} \quad (3.6)$$

$$(\rho_{cp})_{nf} \left(\bar{U} \frac{\partial \bar{T}}{\partial \bar{R}} + \bar{W} \frac{\partial \bar{T}}{\partial \bar{Z}} \right) = k_{nf} \left[\frac{\partial^2 \bar{T}}{\partial \bar{R}^2} + \frac{1}{\bar{R}} \frac{\partial \bar{T}}{\partial \bar{R}} + \frac{\partial^2 \bar{T}}{\partial \bar{Z}^2} \right] + Q_0. \quad (3.7)$$

In the wave frame coordinates system (\bar{R}, \bar{Z}) , flow between the two tubes is unsteady. It becomes steady in a reference frame (\bar{r}, \bar{z}) moving with the same speed as the wave moves in the \bar{Z} -direction. The transformations between the two frames are:

$$\bar{r} = \bar{R}, \quad \bar{z} = \bar{Z} - c\bar{t}, \quad \bar{u} = \bar{U}, \quad \bar{w} = \bar{W} - c, \quad \bar{p}(\bar{z}, \bar{r}, \bar{t}) = \bar{P}(\bar{Z}, \bar{R}, \bar{t}) \quad (3.8)$$

The flow Eqs. (3.4) to (3.7) after using the above transformation can be written as follows

$$\frac{1}{\bar{r}} \frac{\partial (\bar{r}\bar{u})}{\partial \bar{r}} + \frac{\partial \bar{w}}{\partial \bar{z}} = 0, \quad (3.9)$$

$$\begin{aligned} \rho_{nf} \left[\bar{u} \frac{\partial \bar{u}}{\partial \bar{r}} + \bar{w} \frac{\partial \bar{u}}{\partial \bar{z}} \right] &= -\frac{\partial \bar{p}}{\partial \bar{r}} + \mu_{nf} \frac{\partial}{\partial \bar{r}} \left[2 \frac{\partial \bar{u}}{\partial \bar{r}} \right] + \mu_{nf} \frac{2}{\bar{r}} \left(\frac{\partial \bar{u}}{\partial \bar{r}} - \frac{\bar{u}}{\bar{r}} \right) \\ &+ \mu_{nf} \frac{\partial}{\partial \bar{z}} \left[\left(\frac{\partial \bar{u}}{\partial \bar{r}} + \frac{\partial \bar{w}}{\partial \bar{z}} \right) \right], \end{aligned} \quad (3.10)$$

$$\begin{aligned} \rho_{nf} \left[\bar{u} \frac{\partial \bar{w}}{\partial \bar{r}} + \bar{w} \frac{\partial \bar{w}}{\partial \bar{z}} \right] &= -\frac{\partial \bar{p}}{\partial \bar{z}} + \mu_{nf} \frac{\partial}{\partial \bar{z}} \left[2 \frac{\partial \bar{w}}{\partial \bar{z}} \right] + \mu_{nf} \frac{1}{\bar{r}} \frac{\partial}{\partial \bar{r}} \left[\bar{r} \left(\frac{\partial \bar{u}}{\partial \bar{z}} + \frac{\partial \bar{w}}{\partial \bar{r}} \right) \right] \\ &- \sigma B_o^2 (\bar{w} + c) + \rho_{nf} g \alpha (\bar{T} - T_0), \end{aligned} \quad (3.11)$$

$$(\rho_{cp})_{nf} \left(v \frac{\partial \bar{T}}{\partial \bar{r}} + w \frac{\partial \bar{T}}{\partial \bar{z}} \right) = k_{nf} \left[\frac{\partial^2 \bar{T}}{\partial \bar{r}^2} + \frac{1}{\bar{r}} \frac{\partial \bar{T}}{\partial \bar{r}} + \frac{\partial^2 \bar{T}}{\partial \bar{z}^2} \right] + Q_0. \quad (3.12)$$

here \bar{r} and \bar{z} are the coordinates. \bar{z} is taken as the center line of the tube and \bar{r} transverse to it, \bar{u} and \bar{w} are the velocity components in the \bar{r} and \bar{z} directions respectively, \bar{T} is the local temperature of the fluid, p is pressure, B_o is magnetic field. Further, ρ_{nf} is the effective density, μ_{nf} is the effective dynamic viscosity, $(\rho_{cp})_{nf}$ is the heat capacitance, α_{nf} is the effective thermal diffusivity, and k_{nf} is the effective thermal conductivity of the nanofluid, which are defined as

(see refs. [1]).

$$\begin{aligned}
\rho_{nf} &= (1 - \phi) \rho_f + \phi \rho_s, \quad \mu_{nf} = \frac{\mu_f}{(1 - \phi)^{2.5}}, \quad \alpha_{nf} = \frac{k_{nf}}{(\rho c_p)_{nf}}, \\
(\rho c_p)_{nf} &= (1 - \phi) (\rho c_p)_f + \phi (\rho c_p)_s, \\
k_{nf} &= k_f \left(\frac{(1 - \phi) + \frac{2\phi k_{CNT}}{k_{CNT} - k_f} \log\left(\frac{k_{CNT} + k_f}{2k_f}\right)}{(1 - \phi) + \frac{2\phi k_f}{k_{CNT} - k_f} \log\left(\frac{k_{CNT} + k_f}{2k_f}\right)} \right), \tag{3.13}
\end{aligned}$$

where ϕ is the solid volume fraction of the Carbon nanotube. We introduce the following non-dimensional variables:

$$\begin{aligned}
r &= \frac{\bar{r}}{a}, \quad z = \frac{\bar{z}}{\lambda}, \quad w = \frac{\bar{w}}{c}, \quad u = \frac{\lambda \bar{u}}{ac}, \quad p = \frac{a^2 \bar{p}}{c \lambda \mu_f}, \quad \beta = \frac{a}{\lambda}, \quad \theta = \frac{(\bar{T} - \bar{T}_0)}{\bar{T}_0}, \quad t = \frac{c \bar{t}}{\lambda}, \\
M^2 &= \frac{\sigma B_0^2 a^2}{\mu_f}, \quad G_r = \frac{\rho_{nf} g \alpha a^2 \bar{T}_0}{c \mu_f}, \quad \xi = \frac{Q_0 a^2}{k_f \bar{T}_0}. \tag{3.14}
\end{aligned}$$

Making use of these variables defined above in Eqs. (3.9) to (3.12) and using the assumptions of low Reynolds number and long wavelength, the non-dimensional governing equations after dropping the dashes can be written as:

$$\frac{\partial p}{\partial r} = 0, \tag{3.15}$$

$$\frac{dp}{dz} = \frac{1}{(1 - \phi)^{2.5}} \frac{1}{r} \frac{\partial}{\partial r} \left(r \frac{\partial w}{\partial r} \right) - M^2 (w + 1) + G_r \theta, \tag{3.16}$$

$$\frac{1}{r} \frac{\partial}{\partial r} \left(r \frac{\partial \theta}{\partial r} \right) + \xi \left(\frac{(1 - \phi) + \frac{2\phi k_f}{k_{CNT} - k_f} \log\left(\frac{k_{CNT} + k_f}{2k_f}\right)}{(1 - \phi) + \frac{2\phi k_{CNT}}{k_{CNT} - k_f} \log\left(\frac{k_{CNT} + k_f}{2k_f}\right)} \right) = 0, \tag{3.17}$$

here M , ξ and G_r are the Hartmann number, heat absorption parameter and Grashof number respectively. The non-dimensional boundary conditions on the ciliated walls are given as:

$$\frac{\partial w}{\partial r} = 0, \quad \frac{\partial \theta}{\partial r} = 0 \quad \text{at} \quad r = 0, \tag{3.18a}$$

$$w = \frac{-2\pi \epsilon \alpha \beta \cos(2\pi z)}{1 - 2\pi \epsilon \alpha \beta \cos(2\pi z)} - 1, \quad \theta = 0, \quad \text{at} \quad r = h(z) = 1 + \epsilon \cos(2\pi z). \tag{3.18b}$$

here β is the wave number.

3.3 Solutions of the Problem

Since Eqs. (3.15) to (3.17) with boundary conditions (3.18a) and (3.18b) are linear with variable coefficients so their exact solutions for velocity, temperature and pressure gradient can be evaluated by using Mathematica and can be written as follows:

$$w(r, z) = \frac{1}{4M^4(1-\phi)^{\frac{5}{4}}} \left\{ \frac{-M^2(1-\phi)^{\frac{5}{2}} \left(G_r \frac{k_f}{k_{nf}} \xi (r^2 - h^2) + 4 \left(M^2 + \frac{dp}{dz} \right) \right) - 4G_r \frac{k_f}{k_{nf}} \xi + 4I_0 \left(M(1-\phi)^{\frac{5}{4}} r \right) \left[G_r \frac{k_f}{k_{nf}} \xi (2\pi\alpha\beta\epsilon \cos(2\pi z) - 1) + M^2(1-\phi)^{\frac{5}{2}} (2\pi\alpha\beta\epsilon \left(M^2 + \frac{dp}{dz} \right) \cos(2\pi z) - \frac{dp}{dz}) \right]}{I_0 \left(M(1-\phi)^{\frac{5}{4}} h \right) (2\pi\alpha\beta\epsilon \cos(2\pi z) - 1)} \right\}, \quad (3.19)$$

$$\theta(r, z) = \frac{1}{4} \left(\frac{(1-\phi) + \frac{2\phi k_f}{k_{CNT} - k_f} \log \left(\frac{k_{CNT} + k_f}{2k_f} \right)}{(1-\phi) + \frac{2\phi k_{CNT}}{k_{CNT} - k_f} \log \left(\frac{k_{CNT} + k_f}{2k_f} \right)} \right) (h^2 - r^2) \xi, \quad (3.20)$$

The flow rate is given by [34]

$$Q = 2 \int_0^{h(z)} r w dr, \quad (3.21)$$

this implies that

$$\frac{dp}{dz} = \frac{-16h \left(2\pi\alpha\beta\epsilon \cos(2\pi z) \left(G_r \frac{k_f}{k_{nf}} \xi + M^4 (1-\phi)^{\frac{5}{2}} \right) - G_r \frac{k_f}{k_{nf}} \xi \right) I_1 \left(M(1-\phi)^{\frac{5}{4}} h \right) + \left[\begin{array}{l} M(1-\phi)^{\frac{5}{2}} (2\pi\alpha\beta\epsilon \cos(2\pi z) - 1) I_0 \left(M(1-\phi)^{\frac{5}{4}} h \right) \\ \left(M^2(1-\phi)^{\frac{5}{2}} \left(8M^2 (F + h^2) - G_r h^4 \frac{k_f}{k_{nf}} \xi \right) + 8G_r h^2 \frac{k_f}{k_{nf}} \xi \right) \end{array} \right]}{8h^2 M^3 (1-\phi)^{\frac{15}{4}} (1 - 2\pi\alpha\beta\epsilon \cos(2\pi z)) I_2 \left(M(1-\phi)^{\frac{5}{4}} h \right)}. \quad (3.22)$$

where the mean flow rate F is given as follows [34]

$$F = Q - \frac{1}{2} \left(1 + \frac{\epsilon^2}{2} \right). \quad (3.23)$$

Integrating Eq. (3.22) over the interval $[0, 1]$, we can find the pressure rise given by the expression:

$$\Delta P = \int_0^1 \frac{dp}{dz} dz. \quad (3.24)$$

3.4 Results and Discussion

Pictorial representation of the exact solutions, obtained in the previous section, is presented here for clear analysis of the velocity, temperature, pressure gradient and pressure rise. Figs. 3.2(a) display the effect of Hartmann number on the velocity profile. It can be observed that the velocity is symmetric with its center at the center of the tube, and that maximum velocity exists at the center of the tube and it starts decreasing near the ciliated walls. It is also noted that the change in Pure water is more than that of Cu-water as the Hartmann number increases for the single walled carbon nanotubes. Fig. 3.2(b) exhibits that as the velocity profile is directly proportional to the flow rate Q , change in velocity is rapid at the center of the tube and very sluggish near the walls. It is also seen that with an increase in flow rate velocity profile increases for single walled carbon nanotubes.

Effect of increase in the physical parameters ξ and z is shown in Figs. 3.3(a) and 3.3(b). It is seen that the temperature is directly proportional to ξ and inversely proportional to z . The rate of change of temperature in case of Pure water is observed to be very speedy in comparison of Cu-water. Also we see that there is a rise in temperature for heat absorption parameter ξ as compared to coordinate parameter z . Temperature is greater in the center of the tube and it starts decreasing near the walls where it is affected with the metachronal waves of cilia.

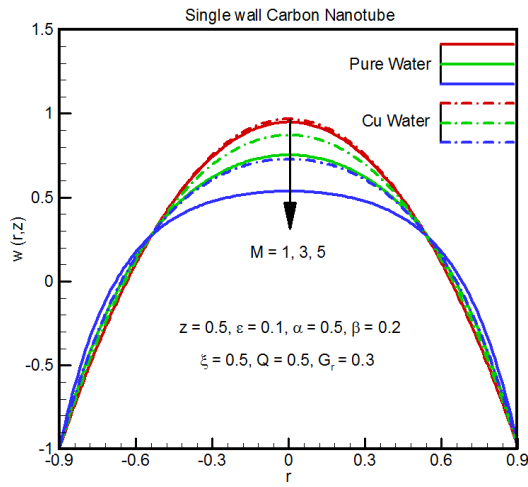
The pressure gradient is represented in Figs. 3.4(a) to 3.4(d) with respect to the axial distance in variation of the Hartmann number and the Grashof number. The graphical illustration depicts that the pressure gradient is directly proportional to the Hartmann number and inversely proportional to the Grashof number. It also implies that the pressure gradient is more in case of the Pure water as compared to the Cu-water for single walled carbon nanotube. The variation in the graphs can be seen more rapid at $z = 0.5$, where the graphs are also symmetric.

In Figs. 3.5(a) to 3.5(d), we have shown the pressure rise against the flow rate Q for different values of Hartmann number M and the non-dimensional cilia length ϵ with respect to Q . It can be seen that pressure rise is directly proportional to the Hartmann number in the pumping region ($\Delta P > 0$) and inversely proportional to the Hartmann number in the augmented pumping region ($\Delta P < 0$). Free pumping region holds for $\Delta P = 0$. Also we note that the pressure rise increases rapidly in case of Cu-water than that of Pure water.

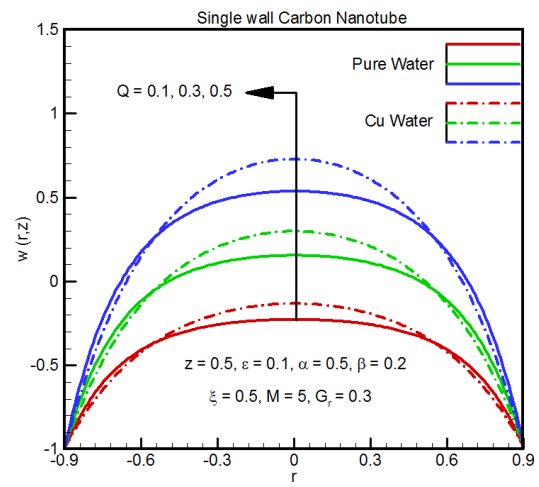
Figs. 3.6(a) to 3.6(d) is the representation of the streamlines for both pure and Cu-water

in case of Single wall carbon nanotube. We see that as the base fluid changes from pure water to Cu-water, the trapped bolus inside the streamlines decreases in size.

Table. 1. Shows the numerical values of velocity profile for SWCNT with the variation of different flow parameters.

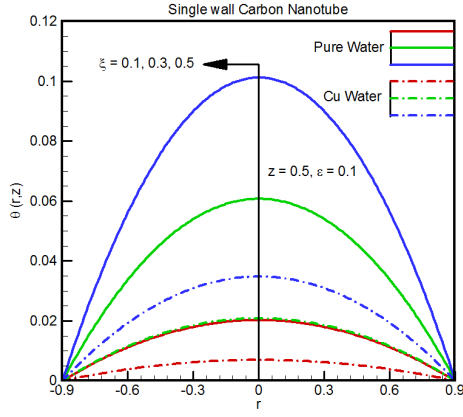


3.2 (a)

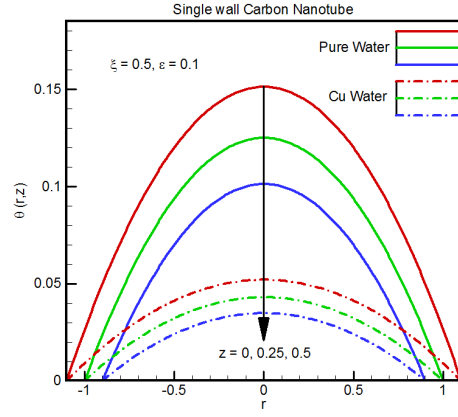


3.2 (b)

Figs. 3.2(a, b). Velocity profile $w(r, z)$ against the radial distance r .

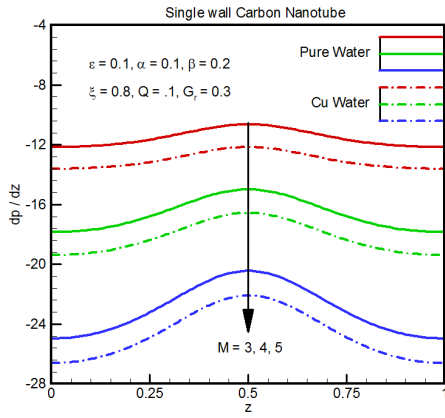


3.3 (a)

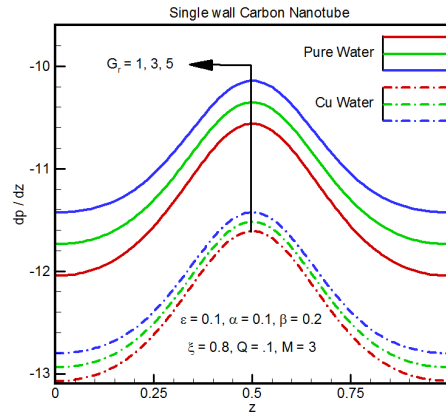


3.3 (b)

Figs. 3.3(a, b). Temperature profile $\theta(r, z)$ against the radial axis r .

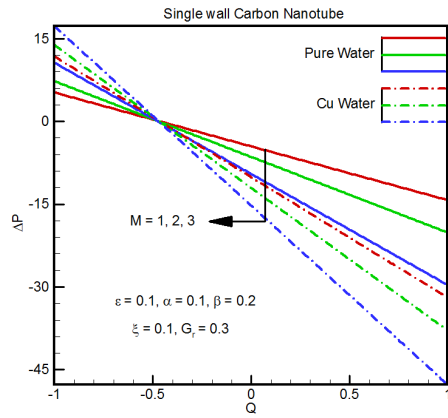


3.4 (a)

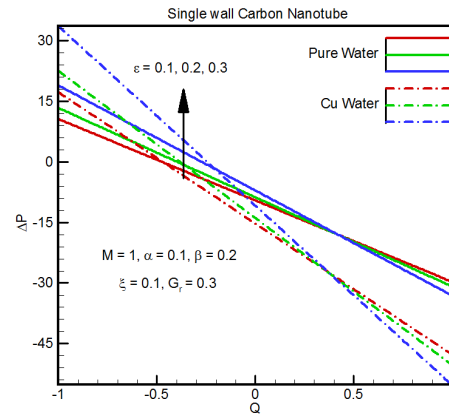


3.4 (b)

Figs. 3.4(a, b). Pressure gradient $\frac{dp}{dz}$ along the tube axis z .

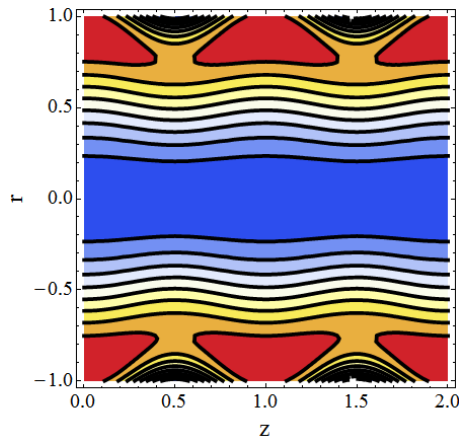


3.5 (a)

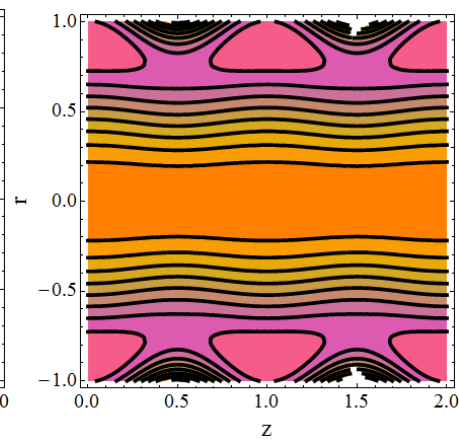


3.5 (b)

Figs. 3.5(a, b).. Pressure rise ΔP against the flow rate Q .



3.6 (a)



3.6 (b)

Figs. 3.6(a, b). Streamlines for velocity profile $w(r, z)$ in comparison between pure H_2O and $Cu-H_2O$ with the interaction of SWCNT.

3.5 Conclusion

Carbon nanotubes suspended nanofluid analysis in a flexible tube with ciliated walls is presented. The analysis of the exact solutions highlights the following aspects.

1) It has been observed that the velocity is symmetric at the center of the tube, and that maximum velocity exists at the center of the tube and it starts decreasing near the ciliated walls.

2) It is also noted that the change in Pure water is greater than that of Cu-water as the Hartmann number increases.

3) The flow rate gives the same physical influence on velocity profile.

4) It is also noted that the rate of temperature change in the case of Pure water is observed to be very fast in comparison with Cu-water.

5) It is also observed that the pressure gradient is greater in case of the Pure water as compared to the Cu-water.

6) As the base fluid changes from Pure water to Cu-water, the trapped bolus inside the streamlines increases in size.

				$w(r, z)$ for <i>SWCNT</i>		
Q	M	G	ϕ	$(r = 0)$	$(r = 0.25)$	$(r = 0.5)$
0.3	2	0.5	0.3	0.448954	0.346236	0.0301363
0.4				0.689394	0.569486	0.200482
0.5				0.929834	0.792735	0.370827
	1			0.968022	0.819977	0.372998
	3			0.872505	0.751464	0.367044
	5			0.729404	0.646104	0.354192
		1		0.729435	0.646127	0.354194
		3		0.729559	0.646217	0.354204
		5		0.729683	0.646307	0.354214
			0	0.54174	0.500762	0.325823
			0.1	0.599364	0.546548	0.336522
			0.2	0.66348	0.596171	0.34612

Table 1. Numerical values of the velocity for single-wall CNT with $\epsilon = 0.1$, $\alpha = 0.1$, $\beta = 0.2$, $\xi = 0.5$, $z = 0.5$.

Chapter 4

A Study of Entropy Generation and Heat Transfer for CNT Suspended Nanofluid in a Porous Ciliated Tube with Permeable Walls

4.1 Introduction

This chapter investigates the entropy generation and convective heat transfer of nanofluids fabricated by the dispersion of single-wall carbon nanotubes (SWCNT) nanoparticles in water as base fluid. The steady flow is induced by Metachronal wave propulsion due to beating cilia. The flow regime is cylindrical porous tube. The flow is restricted under the low Reynolds number and long wavelength approximations. Cilia boundary conditions for velocity components are employed to find the analytical solutions. The impacts of pertinent physical parameters on temperature profile, velocity profile, pressure, entropy, Bejan number and stream lines are computed numerically. A comparative study between SWCNT nanofluids and Pure water is also computed.

4.2 Formulation of the Problem

We consider an incompressible nanofluid in a circular tube with the interaction of single wall carbon nanotube and entropy generation. Inner surface of the circular tube is ciliated with metachronal waves and the flow occurs due to collective beating of cilia. Walls of the tubes are permeable. We represent the geometry of the problem in the cylindrical coordinate system cylindrical (\bar{R}, \bar{Z}) see Fig.4.1.

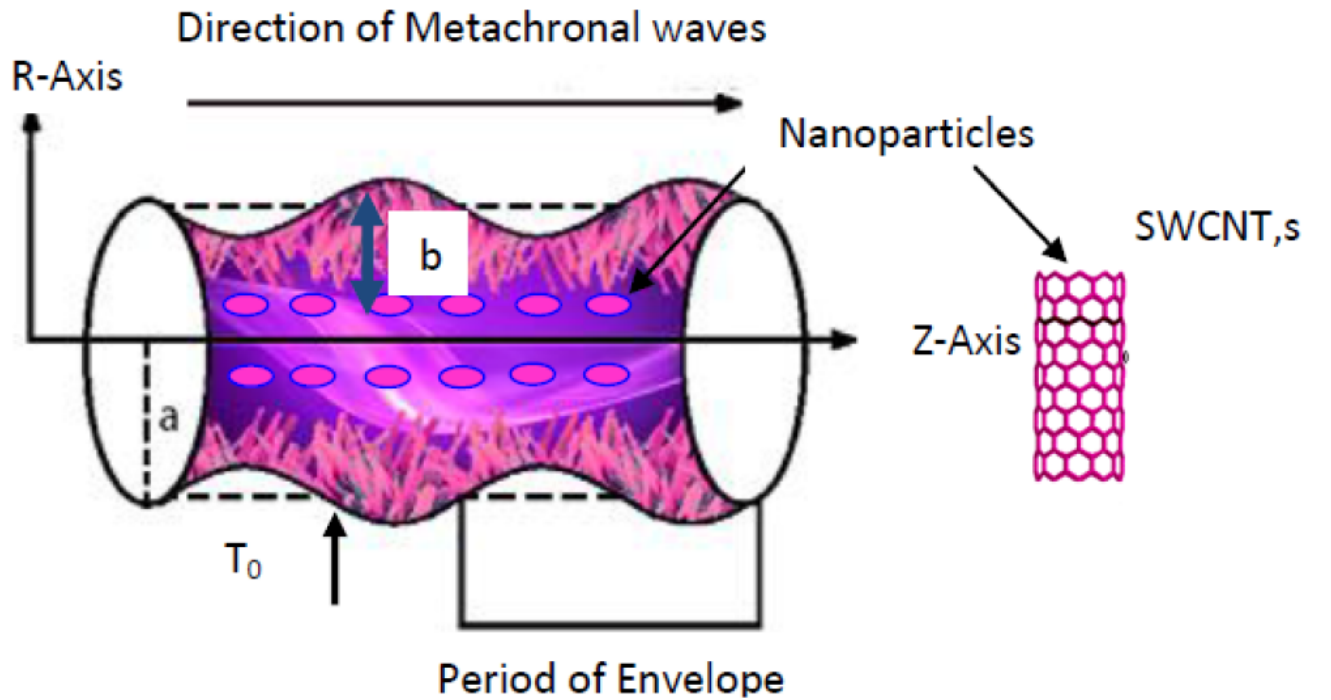


Fig. 4.1. Geometry of the problem.

Envelopes of the cilia tips and velocities of the transporting fluid caused by the cilia tips can be expressed mathematically as defined in Eqs. (3.1) and (3.2).

Following same pattern as done in chapter 3, flow equations in moving frame can be written as follows:

$$\frac{1}{\bar{r}} \frac{\partial (\bar{r}u)}{\partial \bar{r}} + \frac{\partial \bar{w}}{\partial \bar{z}} = 0, \quad (4.1)$$

$$\rho_{nf} \left[\bar{u} \frac{\partial \bar{u}}{\partial \bar{r}} + \bar{w} \frac{\partial \bar{u}}{\partial \bar{z}} \right] = -\frac{\partial \bar{p}}{\partial \bar{r}} + \mu_{nf} \frac{\partial}{\partial \bar{r}} \left[2 \frac{\partial \bar{u}}{\partial \bar{r}} \right] + \mu_{nf} \frac{2}{\bar{r}} \left(\frac{\partial \bar{u}}{\partial \bar{r}} - \frac{\bar{u}}{\bar{r}} \right) + \mu_{nf} \frac{\partial}{\partial \bar{z}} \left[\left(\frac{\partial \bar{u}}{\partial \bar{r}} + \frac{\partial \bar{w}}{\partial \bar{z}} \right) \right], \quad (4.2)$$

$$\begin{aligned} \rho_{nf} \left[\bar{u} \frac{\partial \bar{w}}{\partial \bar{r}} + \bar{w} \frac{\partial \bar{w}}{\partial \bar{z}} \right] &= -\frac{\partial \bar{p}}{\partial \bar{z}} + \mu_{nf} \frac{\partial}{\partial \bar{z}} \left[2 \frac{\partial \bar{w}}{\partial \bar{z}} \right] + \mu_{nf} \frac{1}{\bar{r}} \frac{\partial}{\partial \bar{r}} \left[\bar{r} \left(\frac{\partial \bar{u}}{\partial \bar{z}} + \frac{\partial \bar{w}}{\partial \bar{r}} \right) \right] \\ &\quad - \frac{\mu_{nf}}{K} (\bar{w} + c), \end{aligned} \quad (4.3)$$

$$(\rho c_p)_{nf} \left(\bar{u} \frac{\partial \bar{T}}{\partial \bar{r}} + \bar{w} \frac{\partial \bar{T}}{\partial \bar{z}} \right) = k_{nf} \left[\frac{\partial^2 \bar{T}}{\partial \bar{r}^2} + \frac{1}{\bar{r}} \frac{\partial \bar{T}}{\partial \bar{r}} + \frac{\partial^2 \bar{T}}{\partial \bar{z}^2} \right] + \bar{\Phi}. \quad (4.4)$$

The viscous dissipation term $\bar{\Phi}$ can be obtained from equations of motion [33], i.e.,

$$\bar{\Phi} = \mu_{nf} \left(2 \left(\left(\frac{\partial \bar{u}}{\partial \bar{z}} \right)^2 + \left(\frac{\partial \bar{w}}{\partial \bar{r}} \right)^2 \right) + \left(\frac{\partial \bar{u}}{\partial \bar{r}} + \frac{\partial \bar{w}}{\partial \bar{z}} \right)^2 \right). \quad (4.5)$$

We introduce the following non-dimensional variables:

$$\begin{aligned} r &= \frac{\bar{r}}{a}, \quad z = \frac{\bar{z}}{\lambda}, \quad w = \frac{\bar{w}}{c}, \quad u = \frac{\lambda \bar{u}}{ac}, \quad p = \frac{a^2 \bar{p}}{c\lambda\mu_f}, \quad \beta = \frac{a}{\lambda}, \quad \theta = \frac{(\bar{T} - \bar{T}_0)}{\bar{T}_0}, \\ t &= \frac{c\bar{t}}{\lambda}, \quad D_1 = \frac{K}{a^2}, \quad \text{Pr} = \frac{\mu c_p}{k}, \quad E_c = \frac{c^2}{c_p T_0}, \quad B_r = E_c \text{Pr}. \end{aligned} \quad (4.6)$$

here ϕ is the volume fraction of the carbon nanotube, Pr , B_r are the Prandtl and Brinkman number respectively.

Using the above transformation and using the assumptions of long wavelength and low Reynolds number approximation, the above Eqs. (4.1) and (4.2) takes the form:

$$\frac{\partial p}{\partial r} = 0, \quad (4.7)$$

$$\frac{dp}{dz} = \frac{\mu_{nf}}{\mu_f} \frac{1}{r} \frac{\partial}{\partial r} \left(r \frac{\partial w}{\partial r} \right) - \frac{1}{D_1} \frac{\mu_{nf}}{\mu_f} (w + 1) \quad (4.8)$$

$$\frac{k_{nf}}{k_f} \frac{1}{r} \frac{\partial}{\partial r} \left(r \frac{\partial \theta}{\partial r} \right) + B_r \left(\frac{\mu_{nf}}{\mu_f} \right) \left(\frac{\partial w}{\partial r} \right)^2 = 0. \quad (4.9)$$

The non-dimensional boundary conditions for permeable walls [35] are defined as follows:

$$\frac{\partial w}{\partial r} = 0, \quad \frac{\partial \theta}{\partial r} = 0 \quad \text{at } r = 0, \quad (4.10)$$

$$w = -1 - \frac{-2\pi\epsilon\alpha\beta \cos(2\pi z)}{1 - 2\pi\epsilon\alpha\beta \cos(2\pi z)} - \frac{\sqrt{D_1}}{a_1} \frac{\partial w}{\partial r}, \quad \theta = 0, \quad \text{at } r = h(z) = 1 + \epsilon \cos(2\pi z). \quad (4.11)$$

4.3 Analytic Solutions

Solving Eqs (4.7) to (4.9) together with the boundary conditions in Eqs (4.10) to (4.11), velocity of fluid flow is

$$w(r, z) = -1 - D_1 P + \frac{1}{-1 + 2\pi\epsilon\alpha\beta \cos(2\pi z)} \left\{ \frac{a_1 \sqrt{A}}{I_1\left(\frac{h}{\sqrt{AD_1}}\right)} I_0\left(\frac{r}{\sqrt{AD_1}}\right) \right\}. \quad (4.12)$$

Temperature of the fluid flow is

$$\theta(r, z) = -\frac{B_r k_1^2 (D_1 k_f h^6 + 9 D_1^2 h^4 k_f A)}{576 D_1^3 k_f^2 A} + \frac{B_r k_1^2 r^4}{64 D_1 k_f} + \frac{B_r k_1^2 r^6}{576 D_1^2 k_f A}, \quad (4.13)$$

here

$$A = \frac{\mu_{nf}}{\mu_f}, \quad P = \frac{dp}{dz}, \quad k_1 = \frac{a_1}{I_1\left(\frac{h}{\sqrt{AD_1}}\right) (-1 + 2\pi\epsilon\alpha\beta \cos(2\pi z))}. \quad (4.14)$$

The flow rate is given by

$$Q = 2 \int_0^{h(z)} r w dr, \quad (4.15)$$

here Q [34] is given as follows

$$Q = F + \frac{1}{2} \left(1 + \frac{\epsilon^2}{2}\right). \quad (4.16)$$

Using Eq. (4.12) in eq. (4.15), then solving for $\frac{dp}{dz}$ we get

$$\frac{dp}{dz} = -\frac{1 + \frac{F}{h^2} + \frac{2Ak_1\sqrt{D_1}}{h-2h\pi\alpha\beta\epsilon\cos(2\pi z)}}{D_1}. \quad (4.17)$$

Integrating the Eq. (4.17) over the interval $[0, 1]$, we can find the pressure rise as follows

$$\Delta P = \int_0^1 \frac{dp}{dz} dz. \quad (4.18)$$

4.4 Entropy Generation

The dimensional volumetric entropy generation [33] is defined as

$$S_{gen}''' = \frac{k_{nf}}{\theta_0^2} \left(\left(\frac{\partial \bar{T}}{\partial \bar{r}} \right)^2 + \left(\frac{\partial \bar{T}}{\partial \bar{z}} \right)^2 \right) + \frac{\bar{\Phi}}{\theta_0}. \quad (4.19)$$

Dimensionless form of the entropy generation is given as:

$$N_s = \left(\frac{k_{nf}}{k_f} \right) \left(\frac{\partial \theta}{\partial r} \right)^2 + \theta_0 B_r \left(\frac{\mu_{nf}}{\mu_f} \right) \left(\frac{\partial w}{\partial r} \right)^2, \quad (4.20)$$

here

$$B_r = \frac{c^2 \mu_f}{k_f \bar{T}_0}, \quad \theta_0 = \frac{\bar{\theta}_0}{\bar{T}_0}.$$

Eq. (4.20) consists of two parts, in which the first part is the entropy generation due to finite temperature difference ($N_{s_{cond}}$) and the second part is the entropy generation due to viscous effects ($N_{s_{visc}}$). The Bejan number [28] is defined as

$$Be = \frac{N_{s_{cond}}}{N_{s_{cond}} + N_{s_{visc}}}. \quad (4.21)$$

$$Be = \frac{\left(\frac{k_{nf}}{k_f} \right) \left(\frac{\partial \theta}{\partial r} \right)^2}{\left(\frac{k_{nf}}{k_f} \right) \left(\frac{\partial \theta}{\partial r} \right)^2 + \theta_0 B_r \left(\frac{\mu_{nf}}{\mu_f} \right) \left(\frac{\partial w}{\partial r} \right)^2}. \quad (4.22)$$

4.5 Results and Discussion

In this section, the graphical explanation of the analytical expressions for velocity, temperature, pressure gradient, pressure rise, Entropy generation, Bejan number and stream lines is expressed with respect to certain changes in the physical parameters through the illustrations (Figs. 4.2 to 4.11). A comparative study for Pure water and SWNT-water is also depicted through the numerical results.

Figs. 4.2 (a and b) represent the change in the velocity profile of the fluid flow with respect to slip parameter (a_1) and Darcy number (D_1). It is observed that velocity is directly proportional to both the physical parameters that means we increase the magnitude of the above parameters, the velocity profile will also increase. It attains its maximum values at the center of the tube

and decreases near the boundary of the tube. We also note that the change in the velocity profile with respect to slip parameter (a_1) is greater as compared to Darcy number (D_1). It is further revealed that the variation in velocity profile for SWCNT- nanofluids is more than Pure water at fixed values of other parameters.

The effects of Brinkman number (B_r) and Darcy number (D_1) are shown in the Figs. 4.3(a and b). It can be seen that temperature is directly proportional in both cases. The rate of temperature change in case of SWCNT-nanofluids is observed to be very fast in comparison with Pure water. The temperature is maximum at the center of the tube and it starts decreasing towards the boundary walls.

Figs. 4.4 (a to d) illustrate the pressure gradient against the axial tube length. Figs. 4.4 (a and b) represent the change in the pressure gradient profile of the fluid flow with respect to slip parameter (a_1) and Darcy number (D_1). It is found that the pressure gradient is inversely proportional to slip parameter (a_1). If we increase the parameter D_1 , the change in profile is also going to increase near the walls while the profile is decreasing near the center of the tube. It is clearly pointed out from Figs. 4.4 (c and d) that pressure gradient is inversely proportional to flow rate (Q) while directly proportional to eccentricity of the elliptical motion (α). It is also revealed that the variation in pressure gradient profile with respect to flow rate (Q) is greater as compared to elliptical motion (α). In all the cases, the maximum pressure gradient lies at center of tube length ($z = 0.5$). Pressure gradient is less for SWCNT-nanofluids in comparison to base fluid.

The variation of pressure rise against the flow rate is shown in Figs. 4.5(a-c) under the influence of slip parameter (a_1), Darcy number (D_1) and eccentricity of the elliptical motion (α). It is noticed that pressure for Pure water is more than that of SWCNT nanofluids. Fig. 4.5(a) depicts that pressure diminishes with increasing the magnitude of slip parameter. Fig. 4.5(b) reveals that the pressure increases with increasing the value of Darcy number in the pumping region ($\Delta p > 0$), reverse trend is noticed in augmented pumping region ($\Delta p < 0$) and constant value at free pumping region ($\Delta p = 0$). There is no valuable effect of eccentricity of the elliptical motion on pressure.

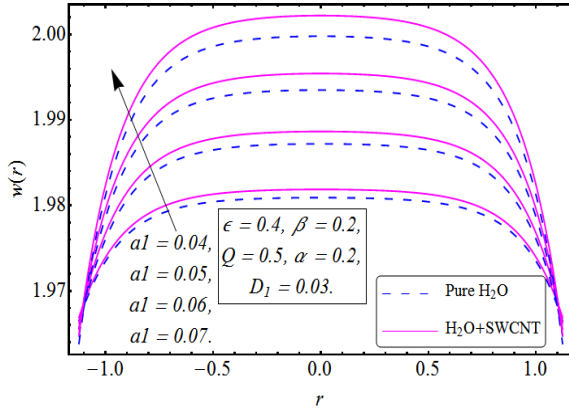
The variation in entropy generation (Ns) against the radial coordinate (r) is illustrated through the Figs. 4.6(a and b) under the influence of Brinkman number (B_r) and Darcy

number (D_1). It is found that the curves are parabolic upward. It is also observed that entropy generation enhances with increasing the magnitude of both parameters i.e. Brinkman number and Darcy number. It is further depicted that attains its maximum value at the walls and minimum value at the center of the tube. The interesting observation is that the change in for the case SWCNT-nanofluids with changes in is slightly differ from Pure water.

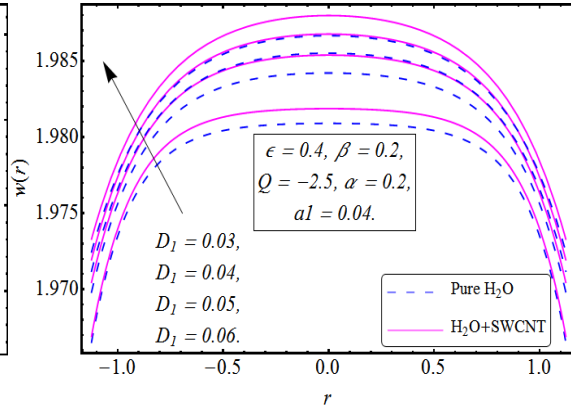
The changes in Bejan number (Be) against the radial coordinate (r) are observed with effects of Brinkman number (B_r) and Darcy number (D_1) through the Figs. 4.7(a and b). It is remarked that the changing nature is parabolic i.e. at zero radial deformation, it is minimum and when it moves positive or negative directions, value of Bejan number (Be) increases. It can also be seen that is directly proportional to Bejan number (Be) and the changes in Bejan number (Be) are greater in SWCNT-nanofluids as compared to Pure water.

A very interesting pumping phenomenon named as trapping and defined as the process of circulation of stream lines at some particular value of flow rate. The stream lines in the wave frame (obeying the Cauchy-Riemann equations $w = \frac{1}{r} \frac{\partial \psi}{\partial r}$ and $u = -\frac{1}{r} \frac{\partial \psi}{\partial z}$) are plotted through Figs. (4.8 to 4.11) to study the impacts of Darcy number (D_1) and slip parameter (a_1) on trapping phenomenon for SWCNT-nanofluids and also base fluid. For Pure water the graphs are shown in Figs. 4.8(a to c) and for SWCNT-nanofluids the graphs are plotted in Figs. 4.9(a to c) with variation of Darcy number. It is predicted that with increment in Darcy number, the trapped bolus inside the streamlines are going to decreases in size in case of Pure water as well as for SWCNT- nanofluids. But when we compare the size of boluses for pure water and SWCNT- nanofluids, trapped bolus is smaller in size for Pure water than that of SWCNT-nanofluids.

The effects of slip parameter (a_1) on streamlines for Pure water and SWCNT-nanofluids are drawn through the Figs. 4.10(a to c) and Figs. 4.11(a to c) respectively. It is revealed that with increases, the value of slip parameter, the trapped bolus inside the streamlines enhances in size while the number of bolus reduces in both cases (Pure water and SWCNT-nanofluids).

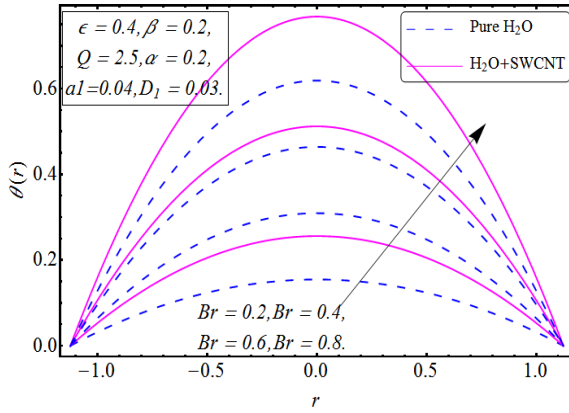


4.2 (a)

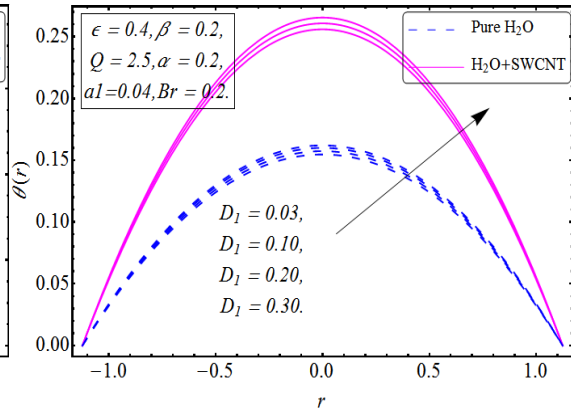


4.2 (b)

Figs. 4.2. Velocity profile (axial velocity against the radial coordinate).

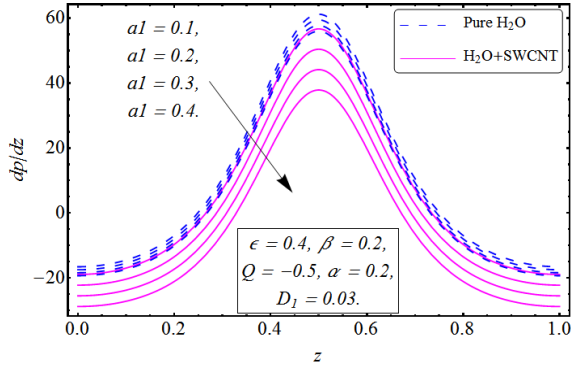


4.3 (a)

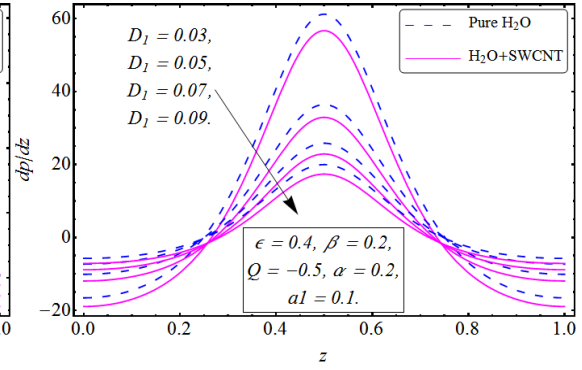


4.3 (b)

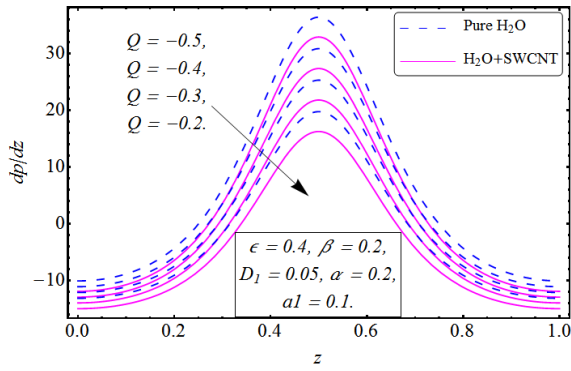
Figs. 4.3. Temperature profile $\theta(r, z)$ against the radial axis r .



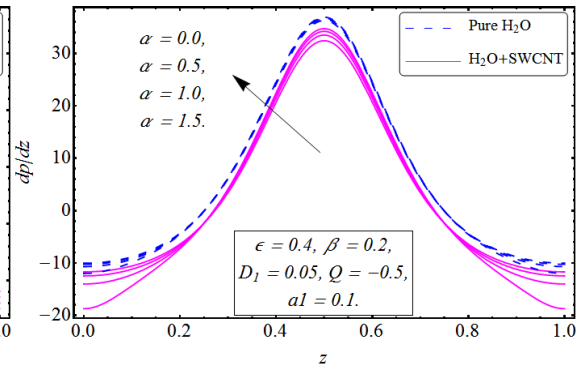
4.4 (a)



4.4 (b)

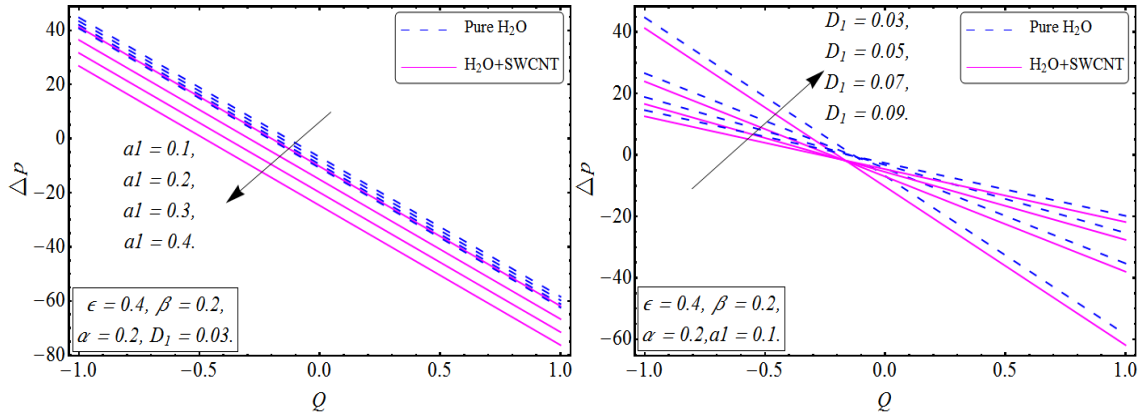


4.4 (c)



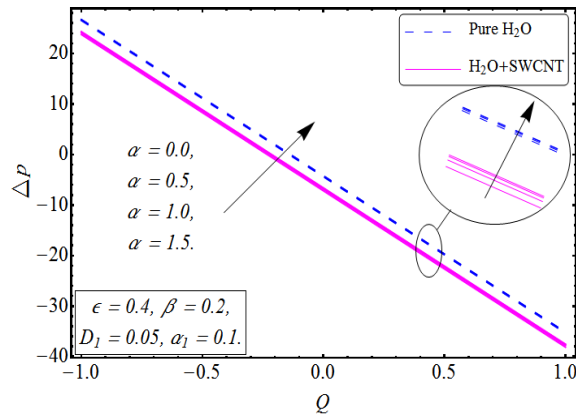
4.4 (d)

Figs. 4.4. Pressure gradient along the tube length.



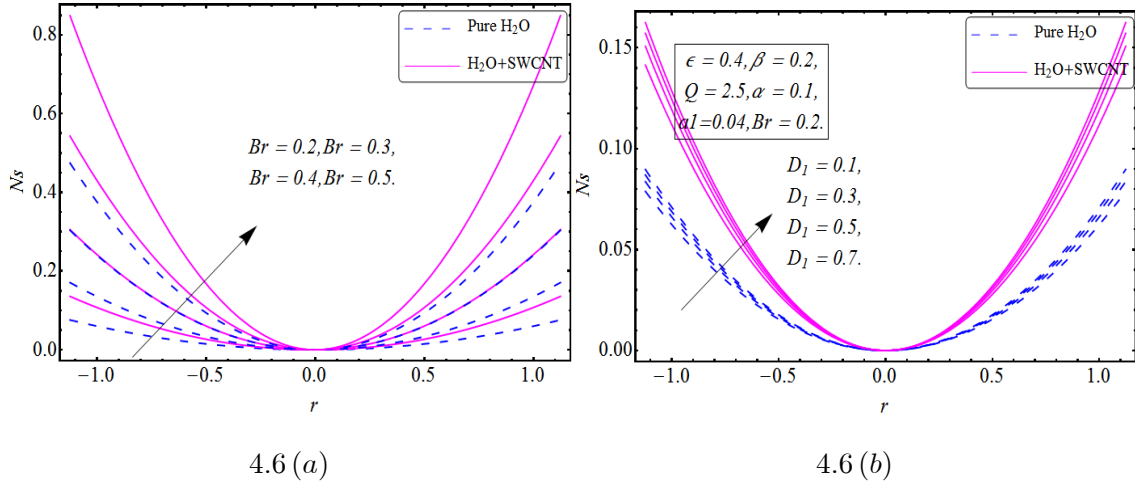
4.5 (a)

4.5 (b)

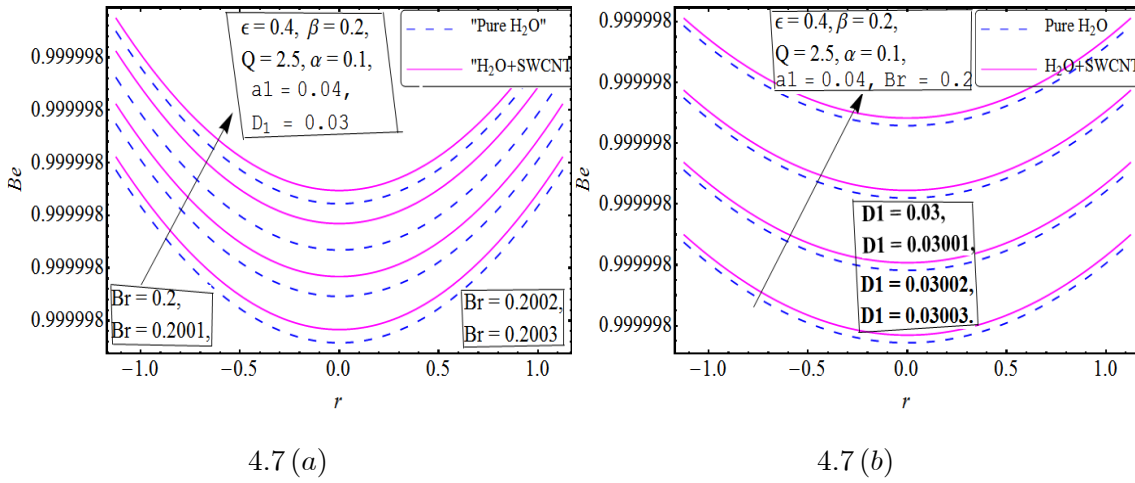


4.5 (c)

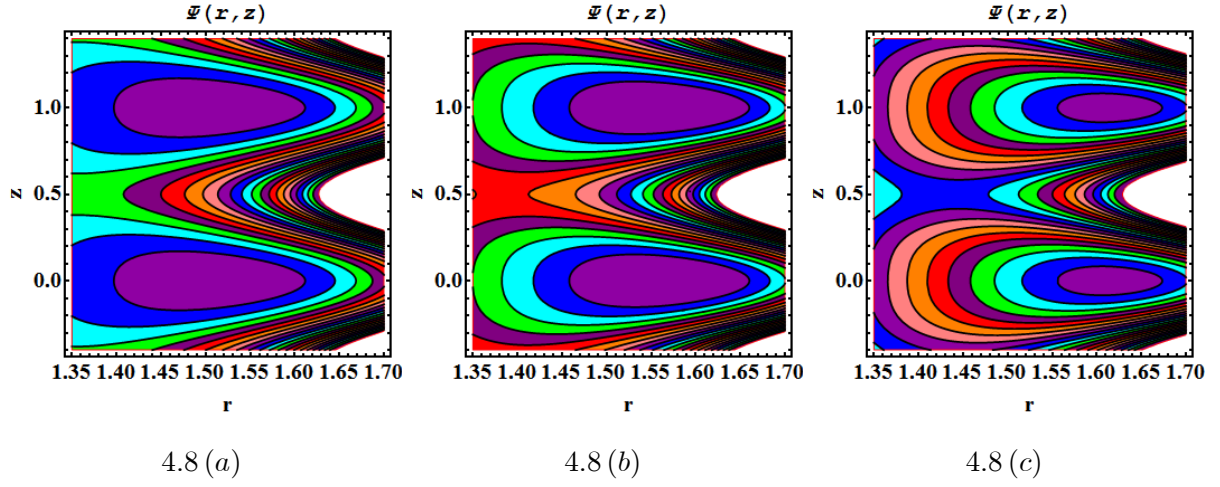
Figs. 4.5. Pressure rise ΔP against the flow rate Q .



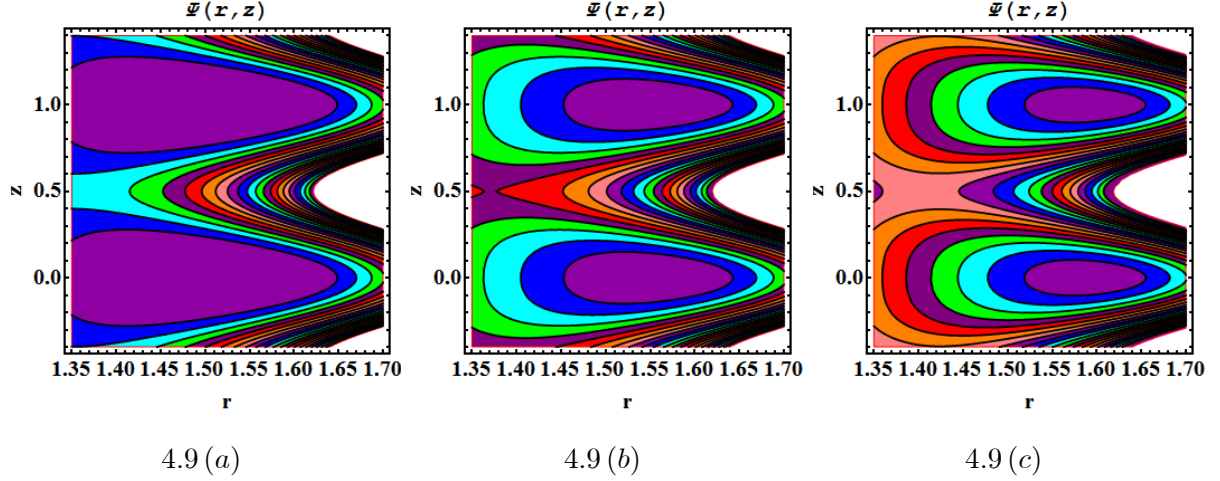
Figs. 4.6. Entropy generation Ns against the radial axis r .



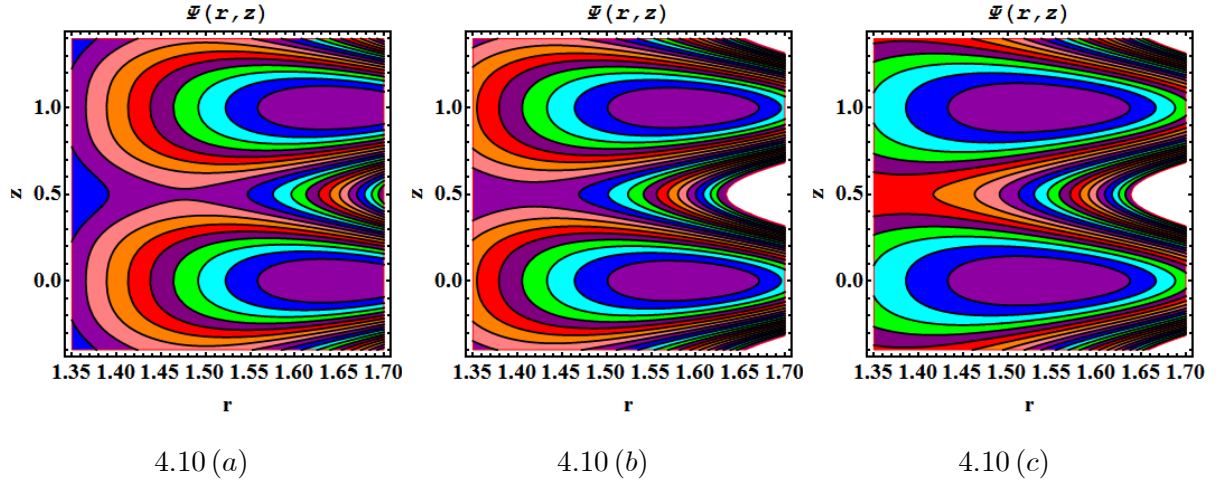
Figs. 4.7. Bejan number Be against the radial axis r .



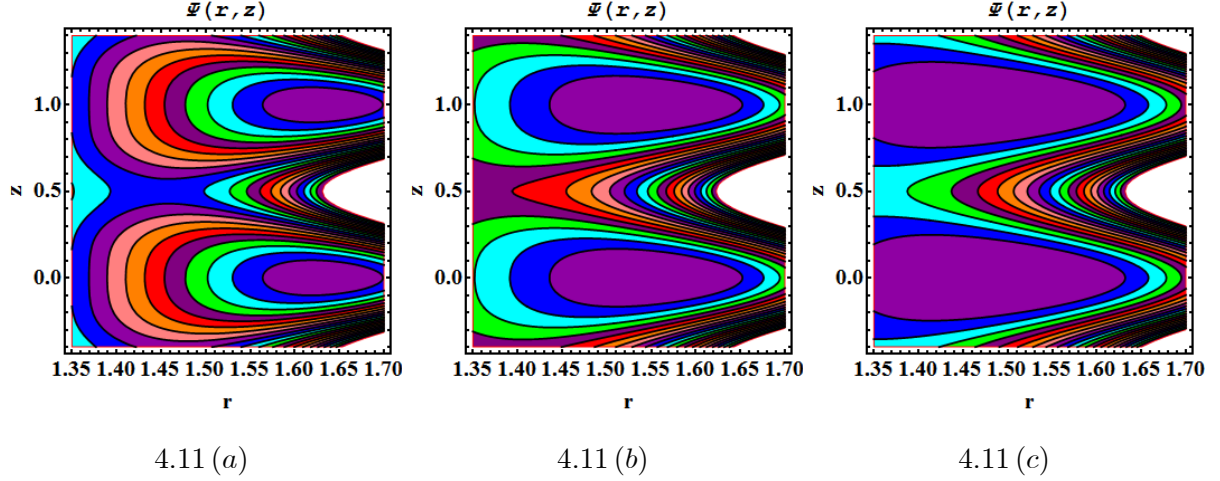
Figs. 4.8. Streamlines for velocity profile $w(r, z)$ for Pure water with varying $D_1 = 0.2, 0.4, 0.6$. Other parameters are $a_1 = 0.2, \epsilon = 0.4, \beta = 0.3, \alpha = 0.3, \phi = 0.3, Q = 2$.



Figs. 4.9. Streamlines for velocity profile $w(r, z)$ for SWCNT with varying $D_1 = 0.2, 0.4, 0.6$. Other parameters are $a_1 = 0.2, \epsilon = 0.4, \beta = 0.3, \alpha = 0.3, \phi = 0.3, Q = 2$.



Figs. 4.10. Streamlines for velocity profile $w(r, z)$ for Pure water with varying $a_1 = 0.1, 0.2, 0.3$. Other parameters are $D_1 = 0.4, \epsilon = 0.4, \beta = 0.3, \alpha = 0.3, \phi = 0.3, Q = 2$.



Figs. 4.11. Streamlines for velocity profile $w(r, z)$ for SWCNT with varying $a_1 = 0.1, 0.2, 0.3$. Other parameters are $D_1 = 0.4, \epsilon = 0.4, \beta = 0.3, \alpha = 0.3, \phi = 0.3, Q = 2$.

4.6 Conclusion

The effects of pertinent physical parameters on entropy generation and heat transfer of CNT nanofluids in flow driven by metachronal wave generated by beating of cilia are computed and discussed in details. On the basis of above discussion, some novel findings are summarized as:

1. Velocity field enhances with increasing the magnitude of slip parameter and Darcy number and it is more for SWCNT- nanofluids than that of Pure water.
2. Pressure gradient is increasing function directly proportional to eccentricity of the elliptical motion whereas decreasing nature with flow rate.
3. Temperature goes up with increasing the magnitude of Brinkman number and Darcy number. The temperature is higher for SWCNT nanofluids in comparison to Pure water.
4. The entropy generation enhances with rising the value of both parameters Brinkman number and Darcy number. It is more for SWCNT nanofluids.
5. The changes in Bejan number is parabolic in nature with radial deformation and it elaborates with increasing the value of both parameters Brinkman number and Darcy number.
6. Bejan number is more for SWCNT-nanofluids as compared to Pure water.
7. The size of trapped bolus expands with increasing the value of slip parameter whereas it contracts with increasing the Darcy number.
8. The Size of trapped bolus for Pure water is smaller than that of the SWCNT-nanofluids.

References

1. H. Xie, H. Lee, W. Youn, and M. Choi, Nanofluids containing multiwalled carbon nanotubes and their enhanced thermal conductivities, *J. Appl. Phys.* 94(8) (2003) 15.
2. M. Liu, M. Ching-Cheng Lin, I-Te Huang, C. Wang, Enhancement of thermal conductivity with carbon nanotube for nanofluids, *Int. Commun. in Heat Mass Transf.* 32(2005)1202 – 1210.
3. Y. Ding, H. Alias, D. Wen, Richard A. Williams, Heat transfer of aqueous suspensions of carbon nanotubes (CNT nanofluids), *Int. J. Heat and Mass Transf.* 49(2006)240 – 250.
4. H. Xie, L. Chen, Review on the Preparation and Thermal Performances of Carbon Nanotube Contained Nanofluids, *J. Chem. Eng. Data* 56 (2011) 1030 – 1041.
5. S. M. Sohel Murshed, C. A. Nietode Castro, Superior thermal features of carbon nanotubes-based nanofluids – A review, *Ren. and Sust. Energy Reviews* 37(2014)155 – 167.
6. S. Halelfadl, T. Maré, P. Estellé, Efficiency of carbon nanotubes water based nanofluids as coolants, *Exp. Ther. and Fluid Sci.* 53(2014)104 – 110.
7. Z. Saida, R. Saidura, N.A. Rahim, M.A. Alim, Analyses of exergy efficiency and pumping power for a conventional flat plate solar collector using SWCNTs based nanofluid, *Energy and Buildings* 78(2014)1 – 9.
8. N. Hordy, D. Rabilloud, J.-Luc Meunier, S. Coulombe, High temperature and long-term stability of carbon nanotube nanofluids for direct absorption solar thermal collectors, *Solar Energy* 105(2014)82 – 90.
9. D. Yadav, R. Bhargava, G. S. Agrawal, Nirmal Yadav, Jinho Lee, M. C. Kim, Thermal instability in a rotating porous layer saturated by a non-Newtonian nanofluid with thermal conductivity and viscosity variation, *Microfluid Nanofluid* (16)(2014)425 – 440.
10. R. Walvekar, M. K. Siddiqui, S. S. Onga and A. F. Ismailc, Application of CNT nanofluids in a turbulent flow heat exchanger, *J. Experim. Nanosci.* 2015 in press.

11. X. Meibo, Y. Jianlin, W. Ruixiang, Thermo-physical properties of water-based single-walled carbon nanotube nanofluid as advanced coolant, *Appl. Therm. Eng.* 87(2015)344–351.
12. N. S. Akbar, A. W. Butt , CNT suspended nanofluid analysis in a flexible with ciliated walls, *Eur. Phys. J. Plus* 129(2014)174 – 184.
13. T. J. Lardner, W. J. Shack, Cilia Transport, *Bull Math Biophys.* 34(1972)25 – 35.
14. M. A. Sleight, *The Biology of Cilia and Flagella*, MacMillian, New York (1968).
15. M. A. Sleight, Patterns of Ciliary Beating, In *Aspects of Cell Motility*, Soc Expl Biol Sump XX I I, Academic Press, New York (1968).
16. J. R. Blake, A note on the image system for a Stokeslet in a no-slip boundary. *Math. Proc. Cambridge Phil. Soc.* 70(02) (1971) 303 – 310.
17. J. R. Blake, A model for the micro-structure in ciliated organisms, *J. Fluid Mech.* 55(01) (1972) 1–23.
18. S. N. Khaderi and P. R. Onck, Fluid structure interaction of three-dimensional magnetic artificial cilia, *J. Fluid Mech.* 708(2012)303 – 328.
19. S. N. Khaderi, M. G. H. M. Baltussen, P. D. Anderson, J. M. J. Den Toonder, & P. R. Onck, The breaking of symmetry in microfluidic propulsion driven by artificial cilia. *Phys. Rev. E.* 82(2010)027302.
20. S. N. Khaderi, J. M. J. Den Toonder, & P. R. Onck, Microfluidic propulsion by the metachronal beating of magnetic artificial cilia: a numerical analysis. *J. Fluid Mech.* 688 (2011) 44 – 65.
21. Y. A. Cengel, and M. A. Boles, *Thermodynamics an Engineering Approach*, Second edition, McGraw Hill, New York 1(994).
22. A. Bejan., A study of entropy generation in fundamental convective heat transfer, *ASME J. Heat Transf.* 101(1979)718 – 725.

23. A. Bejan, The concept of irreversibility in heat exchanger design: counter flow heat exchangers for gas-to-gas applications, *ASME J. Heat Transf.* 99(1977)374 – 380.
24. A. Bejan, Entropy generation minimization: The new thermodynamics of finite-size devices and finite-time processes, *J. Appl. Phys.* 79(1996)(3).
25. A. C. Baytas, Entropy generation for natural convection in an inclined porous cavity, *Int. J. Heat Mass Transf.* 43(2000)2089 – 2099.
26. S. H. Tasnim, M. Shohel, M.A.H. Mamun, Entropy generation in a porous channel with hydromagnetic effect, *Exergy, an Int. J.* 2(2002)300 – 308.
27. S. Mahmud, R. A. Fraser, Magnetohydrodynamic free convection and entropy generation in a square porous cavity, *Int. J. Heat Mass Transf.* 47(2004)3245 – 3256.
28. E Abu-Nada, Numerical prediction of entropy generation in separated flows, *Entropy* 7(2005)234 – 252.
29. H. F. Oztop, A. Z. Sahin, I. Dagtekin, Entropy Generation Through Hexagonal Cross-Sectional Duct for Constant Wall Temperature in Laminar Flow, *Int. J. Energy Res.* 28(8)(2004)725 – 737.
30. I. Dagtekin, H. F. Oztop, A. Z. Sahin, An Analysis of Entropy Generation through Circular Duct with Different Shaped Longitudinal Fins of Laminar Flow, *Int. J. Heat Mass Transf.* 48(1)(2005)171 – 181.
31. I. Dagtekin, H. F. Oztop, A. Bahloul, Entropy Generation for Natural Convection in <GAMMA>-Shaped Enclosures , *Int. Comm. Heat Mass Transf.* 34(2007)502 – 510.
32. H.F. Oztop, K. Al-Salem, A Review on Entropy Generation in Natural and Mixed Convection Heat Transfer for Energy Systems, *Ren. Sust. En. Reviews* 16(1)(2012)911 – 920.
33. M. Pakdemirli and B. S. Yilbas, Entropy generation in a pipe due to non-Newtonian fluid flow: Constant viscosity case, *Sadhana* 31(2006)21 – 29.
34. N. S. Akbar, Entropy generation and energy conversion rate for the peristaltic flow in a tube with magnetic field, *Energy* 82(2015)23 – 30.

35. N. S. Akbar, Ferromagnetic CNT suspended H_2O+Cu nanofluid analysis through composite stenosed arteries with permeable wall, *Physica E: Low-dimensional Systems and Nanostructures* 72(2015)70 – 76.
36. S. Nadeem and H. Sadaf, Theoretical analysis of Cu-blood nanofluid for metachronal wave of cilia motion in a curved channel. *Transaction on Nanobiosciences* 14(2015)447 – 454.